TOXICOLOGICAL SCIENCES **138(2)**, 365–378 2014
doi: 10.1093/toxsci/kfu008
Advance Access publication January 15, 2014

C_{60} Exposure Augments Cardiac Ischemia/Reperfusion Injury and Coronary Artery Contraction in Sprague Dawley Rats

Leslie C. Thompson,[*,1] Rakhee N. Urankar,[*,1] Nathan A. Holland,[*] Achini K. Vidanapathirana,[*] Joshua E. Pitzer,[†] Li Han,[‡] Susan J. Sumner,[‡] Anita H. Lewin,[‡] Timothy R. Fennell,[‡] Robert M. Lust,[*] Jared M. Brown,[†] and Christopher J. Wingard[*,2]

*Department of Physiology, Brody School of Medicine, East Carolina University, Greenville, North Carolina 27834; †Department of Pharmacology & Toxicology, Brody School of Medicine, East Carolina University, Greenville, North Carolina 27834; and ‡Department of RTI International, Research Triangle Park, North Carolina 27709

[1]Authors contributed equally.
[2]To whom correspondence should be addressed at Department of Physiology, Brody School of Medicine at East Carolina University, 600 Moye Blvd, Brody 6N98, Greenville, NC 27834. Fax: (252) 744-3460. E-mail: wingardc@ecu.edu.

Received July 25, 2013; accepted January 9, 2014

The potential uses of engineered C_{60} fullerene (C_{60}) have expanded in recent decades to include industrial and biomedical applications. Based on clinical findings associated with particulate matter exposure and our data with multi-walled carbon nanotubes, we hypothesized that ischemia/reperfusion (I/R) injury and pharmacological responses in isolated coronary arteries would depend upon the route of exposure and gender in rats instilled with C_{60}. Male and female Sprague Dawley rats were used to test this hypothesis by surgical induction of cardiac I/R injury *in situ* 24 h after intratracheal (IT) or intravenous (IV) instillation of 28 μg of C_{60} formulated in polyvinylpyrrolidone (PVP) or PVP vehicle. Serum was collected for quantification of various cytokines. Coronary artery segments were isolated for assessment of vasoactive pharmacology via wire myography. Both IV and IT exposure to C_{60} resulted in expansion of myocardial infarction in male and female rats following I/R injury. Serum-collected post-I/R showed elevated concentrations of interleukin-6 and monocyte chemotactic protein-1 in male rats exposed to IV C_{60}. Coronary arteries isolated from male rats exposed to IT C_{60} demonstrated augmented vasocontraction in response to endothelin-1 that was attenuated with Indomethacin. IV C_{60} exposure resulted in impaired acetylcholine relaxation in male rats and IT C_{60} exposure resulted in depressed vasorelaxation in response to sodium nitroprusside in female rats. Based on these data, we conclude that IT and IV exposure to C_{60} results in unique cardiovascular consequences that may favor heightened coronary resistance and myocardial susceptibility to I/R injury.

Key words: **fullerene; nanotoxicology; myocardial infarction; cytokines; acetylcholine; endothelin-1.**

The heart may be susceptible to infarction in response to ischemia/reperfusion (I/R) injury following pulmonary exposure to multiple types of nanosized particles (< 100 nm). We have previously reported that post-I/R myocardial infarction worsens in a dose- and time-dependent manner following intratracheal (IT) instillation of multi-walled carbon nanotubes (Urankar *et al.*, 2012), cerium oxide nanoparticles (Wingard *et al.*, 2010), or ultrafine particulate matter (Cozzi *et al.*, 2006). Cardiovascular detriments associated with ultrafine particulate matter may result from pulmonary inflammation, oxidative stress, or direct particle effects following translocation (Campen *et al.*, 2012; Utell *et al.*, 2002). Exposure to nanosized particles can result in systemic release of interleukin-6 (IL-6), IL-1β, and tumor necrosis factor-α (TNF-α), as well as increased release of endothelin-1 (ET-1) (Delfino *et al.*, 2005; Du *et al.*, 2013; Gustafsson *et al.*, 2011; Park *et al.*, 2010). Decreased release of nitric oxide (NO) and hypercoagulability associated with exposure to engineered nanomaterials may contribute to impaired perfusion to zones of the myocardium, potentially increasing propensity for cardiac arrhythmia and myocardial infarction. We have also demonstrated that hearts isolated from rats 1 day post-IT instillation of multi-walled carbon nanotubes were prone to premature ventricular contractions, depressed coronary flow during postischemic reperfusion, increased ET-1 release during reperfusion and expansion of post-I/R myocardial infarction (Thompson *et al.*, 2012). That study also suggested that cyclooxygenase (COX) may have contributed to enhanced vascular tone in response to ET-1 in coronaries isolated from the multi-walled carbon nanotube group. It is unclear at this time whether these cardiovascular endpoints are unique to pulmonary routes of exposure or only occur in response to multi-walled carbon nanotubes.

C_{60} fullerene (C_{60}) is a spherical carbon allotrope first generated synthetically in 1985 but has likely been produced naturally in Earth's environment for thousands of years, suggesting that human exposure to C_{60} is not necessarily a novel interaction (Baker *et al.*, 2008). Synthetic production of C_{60} on a commercial scale has increased the probability of human exposures

Disclaimer: The authors are responsible for the conclusions described in this article, which may not represent those drawn by the National Institute of Environmental Health Sciences, East Carolina University or RTI International.

© The Author 2014. Published by Oxford University Press on behalf of the Society of Toxicology.
All rights reserved. For permissions, please email: journals.permissions@oup.com

occupationally and potentially even environmentally (Kubota *et al.*, 2011). The growing number of industrial and medical applications for C_{60} is not surprising due to its unique physicochemical properties (Morinaka *et al.*, 2013). The medicinal uses for C_{60} spur from its capacity to function as an antiviral, photosensitizer, antioxidant, drug/gene delivery device, and contrast agent in diagnostic imaging (Bakry *et al.*, 2007). C_{60} has been found in occupational environments at concentrations of 23,856–53,119 particles/L air (Johnson *et al.*, 2010). Given this potential for humans to encounter C_{60}, assessments of *in vitro* cytotoxicity (Bunz *et al.*, 2012; Jia *et al.*, 2005), *in vivo* biodistribution (Kubota *et al.*, 2011; Sumner *et al.*, 2010), biopersistence (Shinohara *et al.*, 2010), and adverse pulmonary responses to C_{60} have been conducted (Baker *et al.*, 2008; Morimoto *et al.*, 2010; Ogami *et al.*, 2011; Shinohara *et al.*, 2011). Despite the effort put into developing a toxicological profile for C_{60}, the potential impacts of C_{60} on the cardiovascular system have rarely been examined.

The purpose of this study was to examine cardiovascular detriments associated with different routes of exposure to C_{60} and to delineate the responses to C_{60} exposure in different genders. We examined the highest C_{60} concentration that we were able to achieve in solution (0.14 μg/μl). Here we delivered 28 μg of C_{60} total, either by IT or IV instillation in rats, a mass smaller than others that have been characterized for C_{60} exposure in rats (Shinohara *et al.*, 2010).

Based on clinical findings associated with particulate matter exposure and our data with multi-walled carbon nanotubes, we hypothesized that I/R injury and pharmacological responses in isolated coronary arteries would depend upon the route of exposure and gender in rats instilled with C_{60}.

MATERIALS AND METHODS

C_{60} fullerene (C_{60}) and vehicle suspensions were formulated, characterized for zeta potential, hydrodynamic size, and transmission electron micrographed by RTI International (Research Triangle Park, NC). Dry C_{60} was purchased from Sigma-Aldrich (St. Louis, MO; Cat no. 379646). Due to its hydrophobicity, C_{60} was formulated with polyvinylpyrrolidone (PVP), and the dried pellets of C_{60}/PVP were suspended in saline. We dissolved PVP in saline to 1.4% for vehicle samples. For more information about our formulation of C_{60} see the Supplementary materials. PVP-coated C_{60} (C_{60}) and PVP vehicles (vehicle) were analyzed for zeta potential and hydrodynamic diameter using a Malvern Zetasizer NanoZS (Malvern Instruments, Worcestershire, UK) with a 633 nm laser source, 173° detection angle, and a clear disposable zeta cell. The following protocol was used to characterize each suspension while at room temperature (25°C) and was designed to mimic the sample preparation for animal exposures. Sterile normal saline (250 μl) was added to the vial containing the C_{60} or vehicle pellets and the vial was immediately placed in the cup horn sonicator and the sample was sonicated at 50% amplitude to obtain total energy output of 8800–9400 J. This process was repeated for two more vials. The contents of the three vials were combined, vortexed for 10 s, and delivered into the Malvern cell for measurement using a syringe. Size and zeta potential measurements were done using a Malvern disposable capillary cell (Malvern Instruments, no. DTS1061C). Measurements were performed in sequence of (1) first size determination, (2) zeta potential measurement, and (3) second size determination to confirm particle size after zeta potential measurement. The sample cell remained undisturbed in the instrument throughout the three measurements, which took ~6–8 min. All experiments were performed in triplicate.

Transmission electron microscopy (TEM) was performed using an FEI Tecnai G^2 Twin (Hillsboro, OR) high-resolution transmission electron microscope at Duke University, Shared Material and Instrument Facility (Durham, NC). C_{60} samples were prepared as described and sonicated in a cuphorn sonicator at 50% amplitude to obtain total energy output of 8880 J. TEM copper grids were dipped into the C_{60}/PVP suspension and dried completely in a well-ventilated fume hood before imaging.

C_{60} particle number was analyzed in solution by counting events in 10 μl of C_{60} sample using a BD Accuri C6 flow cytometer (BD, San Jose CA). Briefly, C_{60} were prepared as described and sonicated for 2 min at 50% amplitude using a QSonica Q700 sonicator (QSonica). Each sample was run through the flow cytometer to collect a total of 10 μl and analyzed for total events using BD Accuri C6 software with background events subtracted. C_{60} samples were analyzed on four separate runs with a cleaning cycle run between each sample measurement. Each measurement was multiplied by 20 to obtain the particle number delivered to each rat (10 μl × 20 = 200 μl). The mean of the triplicate measurement is reported.

Male and female Sprague Dawley rats were purchased from Charles River (Morrisville, NC) at 10–12 weeks of age and housed in the Department of Comparative Medicine at East Carolina University. Rats had access to standard laboratory chow and water *ad libitum* in a temperature-regulated facility (23 ± 1°C) under 12:12 h light-dark cycles. Each rat was provided a minimum of 5 days to acclimate prior to experimental manipulations. All use of rats in this study complied with protocols approved by the East Carolina University Institutional Animal Care and Use Committee.

C_{60} and vehicle exposures in rats were administered intratracheally (IT) or intravenously (IV) into the lateral tail vein under Isoflurane anesthesia. Specifically, lyophilized C_{60} and vehicle pellets were received at East Carolina University in separate vials for each rat. Sterile saline was added to the dry powder in each vial to generate either a 1.4% PVP in saline (vehicle) or 0.14 μg/μl of C_{60} coated with PVP to 1.4% in saline (C_{60}). Immediately prior to administration, the vials of C_{60} and vehicle were sonicated using a Misonix Sonicator 4000 cup horn sonicator (Qsonica, LLC, Newton, CT) for 2 min at 50% amplitude, generating a total of 8885 J of energy. We administered 200 μl

of C_{60} (28.0 μg of C_{60} formulated with PVP) or vehicle to each rat 24 h prior to cardiopulmonary evaluation. Approximate C_{60} dosing was 93.33 μg/kg based on the weight of a 300 g rat.

Right lung bronchoalveolar lavage (BAL) and cell differential analysis was performed by modifying a protocol previously described for mice (Katwa *et al.*, 2012). Rats were anesthetized deeply with Isoflurane and a pneumothorax was induced immediately. The thoracic cage was removed for optimal visualization of the lungs, lower trachea, and main bronchi. The connective tissue surrounding the lung was resected and the left main bronchus was ligated. A tracheotomy was performed allowing an 18 gauge angiocatheter to be inserted and secured with 2–0 suture. One bolus of Hanks balanced saline solution (23.1 ml/kg) was lavaged into the right lung three times successively. Recovered BAL fluid was centrifuged at 1000 × g for 10 min at 4°C. The BAL supernatant was used for protein quantification. The cell pellets were resuspended in 1 ml of fresh Hanks balanced saline solution and total cell counts were determined with a Cellometer Auto X4 (Nexcelom Biosciences, LLC., Lawrence, MA). BAL fluid volumes containing 20,000 cells were centrifuged onto glass slides using a Cytospin IV (Shandon Scientific Ltd, Cheshire, UK) and stained via a three-step hematology stain (Richard Allan Scientific, Kalamazoo, MI). Cell differential counts were determined microscopically based on hematologic stain and cellular morphology. A total of 300 cells per slide were counted to estimate cell percentage.

BAL fluid protein quantification was performed using a standard Bradford protein assay. In short, BAL fluid proteins were quantified using 5 μl of sample diluted 250 μl of Bradford reagent in duplicate wells of using a 96-well plate. Absorbance values were read at 562 nm using a BIO-TEK Synergy HT plate reader (Winooski, VT) and data were analyzed with Gen5 software (BIO-TEK). Absorbance values for each sample were compared with a standard curve generated using 2.0–0.0625 mg/ml bovine serum albumin.

Unlavaged left lung histology was performed by removing the previously placed suture from the left main bronchus and tying off the right main bronchus. An 18 gauge angiocatheter was inserted into the tracheal opening. The tubed trachea and left lung were excised intact and placed in a 20 ml disposable glass vial. The tubing hub was connected to a fixative reservoir that delivered unbuffered zinc formalin (Richard Allan Scientific) at 30 cmH_2O. After inflation the lung was allowed to fix for 24–72 h and then processed and embedded in paraffin. Longitudinal lung sections (8 μm) were mounted on glass slides and stained with hematoxylin and eosin (H&E) for morphological analysis under a light microscope.

Cardiac I/R injury and myocardial infarct size analysis were performed by modifying the protocol we have previously reported using mice (Urankar *et al.*, 2012). I/R experiments were conducted in a cohort of rats separate from those used for BAL, histology, and coronary vascular studies. Twenty-four hours following exposure to C_{60} or vehicle, male and female rats were anesthetized by an intraperitoneal injection of ketamine/xylazine (85/15 mg/kg, respectively) and given supplemental injections throughout the procedure to maintain anesthesia. Body temperature was maintained at 37°C with a heating pad and TC-1000 Temperature Controller (CWE, Inc., Ardmore, PA). Rats were intubated via tracheostomy with a 16 gauge angiocatheter and mechanically ventilated at 81 breaths/min with 100% O_2 using a Harvard Inspira Advanced Safety Ventilator (Holliston, MA). Male rats were ventilated with 3.0 ml tidal volumes and female rats were ventilated with 2.8 ml tidal volumes. A left parasternal thoracotomy was performed and the pericardium was gently removed. The left anterior descending coronary artery (LAD) was identified and ligated ~4 mm distal to its origin between the conus arteriosus and the left atrium with 6–0 prolene suture tied over polyethylene tubing. Effective occlusion of the LAD was confirmed visually by pallor distal to the ligature. After 20 min of ischemia the tubing was removed and reperfusion was allowed for 2 h. One milliliter of blood was drawn from the inferior vena cava at the end of reperfusion for serum analysis.

Determination of post-I/R myocardial infarct size was conducted by replacing the ligature at the original point of occlusion. The aortic arch was cannulated and 1% Evans blue dye was perfused retrograde to delineate the myocardium subjected to I/R from the myocardium perfused throughout the procedure. Hearts were excised and cut serially into 1 mm sections from the point of ligation to the apex. Sections were incubated for 20 min in 0.1–1.0% triphenyltetrazolium chloride (TTC) solution to demarcate infarcted from noninfarcted tissue. TTC is reduced enzymatically to a brick red color in viable tissue, whereas infarcted tissue remains pale. Both sides of all heart sections were digitally imaged. Image J software was downloaded from the National Institutes of Health website (http://rsbweb.nih.gov/ij/) and used to determine the size of the left ventricle (LV), zone at risk and the area of infarction.

Serum collection, coronary artery isolation, and vessel viability assessment were conducted 24 h after IT or IV exposure to C_{60} or vehicle in male and female rats not subjected to I/R. Rats were anesthetized deeply with Isoflurane and a pneumothorax was induced immediately. One milliliter of blood was drawn directly from the right ventricle of the heart for serum analysis and then each animal was exsanguinated by cutting the inferior vena cava. Coronary artery isolation was performed as we have previously described (Thompson *et al.*, 2012). The heart was excised and placed in cold physiological saline solution (PSS); [mM] 140.0 NaCl, 5.0 KCl, 1.6 $CaCl_2$, 1.2 $MgSO_4$, 1.2 3-[N-morpholino]-propane sulfonic acid, 5.6 D-glucose, and 0.02 EDTA (pH 7.4 @ 37°C). Paired segments of the LAD, ~1 mm in length, were dissected away from the LV between the circumflex artery and the first major bifurcation of the LAD. Segments were mounted into chambers of a 610M multichannel wire myograph (DMT, Ann Arbor, MI) using 0.04 mm diameter stainless steel wire. After a 45 min equilibration period, length and lumen diameter were determined using the reticle micrometer of a stereo dissecting scope positioned over the chambers. Resting

tension was established by determining diameter-tension relationships and setting each segment to 90% of the lumen circumference achieved at 13.3 kPa (Halpern and Mulvany, 1977). An additional 45 min equilibration period was allowed and then tissue viability was assessed by potassium depolarization for 7 min with 109mM K^+PSS (equal molar substitution of K^+ for Na^+). LAD segments were relaxed using successive washes with fresh PSS and endothelial integrity was tested by preconstricting with 1.0μM serotonin for 3 min followed by addition of 3.0μM acetylcholine (ACh). Each LAD segment was washed with fresh PSS every 10 min for 30 min before starting experimental pharmacology protocols. Myograph data were recorded in mN and were collected via computer using a PowerLab8/35 data acquisition interface (ADInstruments, Colorado Springs, CO) and LabChart 7 Pro software (ADInstruments). Data from each vessel segment were normalized to the vessel surface area (length × 2 × width) to yield segment stress (mN/mm^2). LAD segments that generated less than 2.0 mN/mm^2 in response to K^+PSS, 1.0 mN/mm^2 in response to 1.0μM serotonin or relaxed less than 70% of the serotonin preconstriction were not considered viable and excluded from further study.

Concentrations of cytokines were analyzed using serum samples collected 24 h following exposure to C_{60} or vehicle. Serum from male and female rats subjected to I/R (Post-I/R) were tested for concentrations of IL-6, monocyte chemotactic protein-1 (MCP-1), vascular endothelial growth factor (VEGF), TNF-α, eotaxin, and IL-1β using a custom Milliplex MAP Cytokine/Chemokine Panel and Immunoassay (EMD Millipore, Billerica, MA). Serum cytokine concentrations collected from male rats subjected to I/R were also compared with serum cytokine concentrations of male rats not subjected to I/R that underwent vascular studies (No-I/R). The assays were run according to the manufacturer's instructions. Assays were analyzed using a Luminex 200 (Luminex, Austin, TX) and results reported using Luminex xPONENT software version 3.1. Any sample concentration that fell below the detection limit of the assay was reported as 0.0 pg/ml.

Pharmacology of the isolated coronary artery (LAD) was evaluated using cumulative concentration-response protocols designed to test endothelial-dependent vasorelaxation, modified from Tawfik *et al.* (2008). Paired LAD segments isolated from IT or IV exposed male and female rats were subjected to cumulative concentrations of serotonin (10nM–3.0μM, 5-HT) and given 3 min to respond at each concentration before proceeding to the next concentration. The coronary artery vascular smooth muscle stress (mN/mm^2) generated in response to 5-HT of paired segments was averaged at each concentration for data reporting. Upon verifying stable tension after addition of the highest concentration of 5-HT, one of the paired segments was subjected to ACh (1.0nM–1.0μM) to assess endothelial-dependent smooth muscle relaxation and the other segment was subjected to cumulative concentrations of NO donor sodium nitroprusside (SNP) (1.0nM–1.0μM) to assess endothelial-independent smooth muscle relaxation. Each LAD segment was given 3 min to respond at each concentration before proceeding to the next concentration.

Coronary artery ET-1 responses were conducted as we previously reported (Thompson *et al.*, 2012). Following ACh and SNP protocols paired LAD segments from each group was subjected to ET-1 concentration-response experiments. These LAD segments were washed with fresh PSS every 10 min for a minimum of 30 min before starting ET-1 protocols. After confirming that basal resting tension had been re-established, one of the paired LAD segments was incubated with 10μM of the nonselective COX inhibitor Indomethacin (Sigma-Aldrich, St. Louis, MO) for 20 min. Indomethacin remained in the preparation throughout the remaining protocol. ET-1 was added cumulatively to each vessel chamber from 0.1nM to 1.0μM and given 7 min to respond at each concentration before the next concentration was applied.

Statistical analysis and data are expressed as mean ± SEM unless otherwise indicated and significant p-values (< 0.05) marked. Graphpad Prism software (version 5, LaJolla, CA) was used to graph and analyze all data. Cardiac I/R data were compared by ANOVA with Dunnett's Multiple Comparison post-tests. Isolated coronary artery vascular response curves were compared using repeated measures ANOVA with Bonferroni's post-tests and nonlinear regression analysis of the four parameter best-fit values (Ludbrook, 1994). Reported EC_{50} and Hills-slope values were derived from normalized fits of each individual LAD concentration-response curve (0–100% of response) and were compared by t-test across treatment within delivery routes and by ANOVA against matched treatments across delivery routes and naïve controls. Statistical power and group size were based on power analysis of our cardiac I/R experiments in order to understand variability in physiological mechanisms that may contribute to any myocardial vulnerability to infarction following C_{60} exposure.

RESULTS

C_{60} Characterization

The physical characteristics of both PVP vehicle and C_{60}/PVP suspensions are outlined in Table 1. Hydrodynamic diameter and polydispersity index (PDI) of the particles in both suspensions were obtained by using CONTIN algorithm. These demonstrate agreement between particle size and dispersity across multiple measurements within each of the C_{60}/PVP and PVP vehicle suspensions. The size and dispersity characteristics varied only slightly over a 38 min testing period despite the fact that a zeta potential in the range of 0–5 mV is indicative of rapid flocculation or coagulation. The small standard deviation indicates that the particles remain well suspended over the 8 min interval between two measurements. Moreover, small difference in hydrodynamic size observed over a 38 min testing period (animal dosing time frame) indicates that the particles are stable during this time frame. TEM of C_{60}/PVP deposited

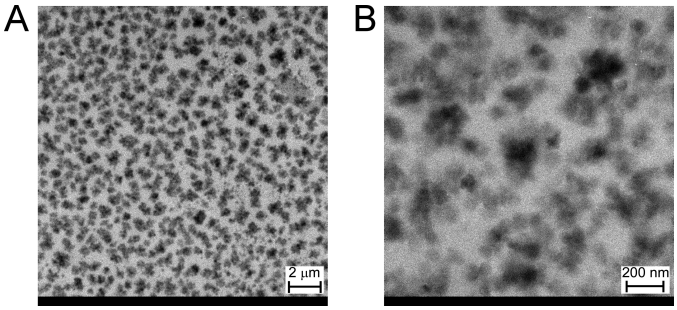

FIG. 1. C_{60} particle size and morphology. TEM of C_{60} samples taken from those used in this study shows (A) at lower magnification C60 aggregates appear to range from ~100 nm to 800 nm in diameter. (B) Higher magnification TEM shows C60 agglomerates ranging from ~50 nm to 200 nm in diameter.

from a suspension prepared as for dosing is presented in Figure 1. A count of 29 separate C60/PVP agglomerates showed an average particle size of 115 nm with a standard deviation of 32 nm. Images of the vehicle suspension under the same magnifications did not show any particles (not shown). The flowcytometery data indicated that there were ~25,791 ± 1351 particles of C_{60}/10 μl of sample. This means that ~515,825 ± 27,014 C_{60} particles were delivered to each rat in the IT and IV C_{60} groups. Based on the assumption that the C_{60}/PVP particles are spherical, we can use the experimentally determined particle size to estimate the total surface area. Use of the DLS-determined hydrodynamic diameter results is a surface area of 0.43 μm^2/particle and use of the TEM determined size gives a surface area of 0.0415 μm^2/particle. Assuming that the particles are discrete, the total estimated surface area should be between 107 ± 5.6 and 1109 ± 58 $\mu m^2/\mu l$. Based on these calculated surface areas, we can further estimate that each rat in the C_{60} group would have been exposed to between 21,400 ± 1120 μm^2 and 221,800 ± 11,600 μm^2.

Pulmonary Histology and Differential Cell Counts

Representative lung morphologies following IT or IV exposure to C_{60} in male rats are presented in Figure 2. Lung histology from female rats is also provided in Supplementary figure 2. Examination of 8 μm lung sections at 10× and 40× revealed no significant inflammation nor differences between Naïve (Fig. 2A) and IT vehicle (Fig. 2B) exposure in male rats. The histology of lung sections from IT C_{60} (Fig. 2C), IV vehicle (Fig. 2D), and IV C_{60} (Fig. 2E) exposures showed minimal inflammation, wall thickening, and cellular infiltrate. BAL protein and differential cell counts are reported in Table 2. Few differences were identified including increased total protein concentrations ($p < 0.05$) in BAL fluid collected from male rats exposed to IV C_{60} compared with IT C_{60} exposed males, and increased number of eosinophils in BAL fluid collected from IT C_{60} females compared with IT vehicle females.

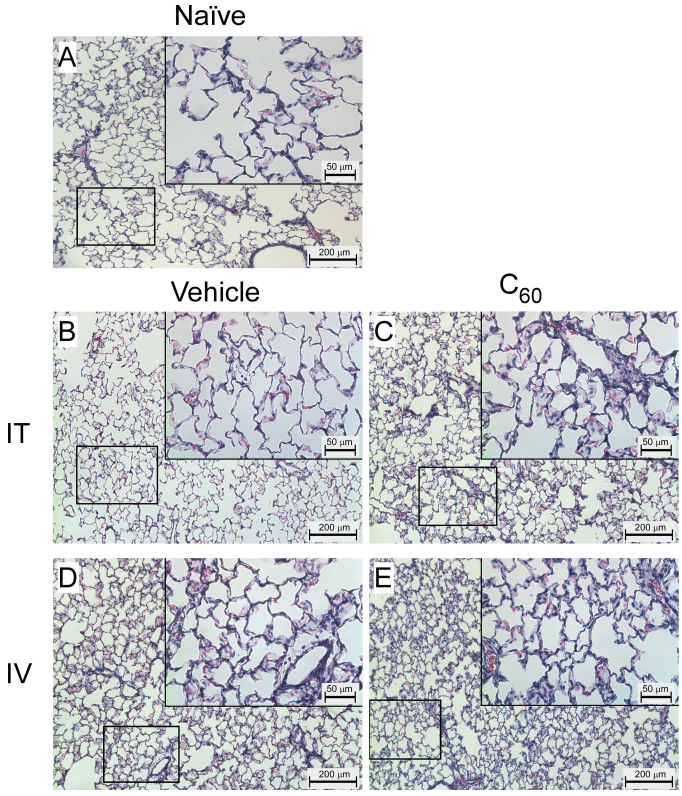

FIG. 2. Male rat left lung histology. To visually assess pulmonary responses to C_{60} exposure in male Sprague Dawley rats, sections of the left lung (8 μm) were stained with H&E and examined by light microscopy at 10× and 40× (inlays) magnification. (A) Representative images from a naïve male rat. (B) Representative images from a male rat intratracheally (IT) exposed to the PVP vehicle. (C) Representative images from a male rat IT exposed to C_{60}. (D) Representative images from a male rat intravenously (IV) exposed to vehicle. (E) Representative images from a male rat IV exposed to C_{60}.

Cardiac I/R Injury

The impact of IT or IV exposure to C_{60} on cardiac I/R injury in male and female rats is represented in Figure 3 (N = 4–5). Following I/R we found expansion of myocardial infarction in male rats exposed to C_{60} suspensions when compared with the infarct size measured in the vehicle groups. Male rats demonstrated no significant differences between the extent of I/R injury across IT or IV exposure routes. Female rats also suffered myocardial infarct expansions following I/R in both C_{60} exposed groups compared with infarct sizes in hearts from vehicle groups. Female rats did show significantly larger myocardial infarctions following IT exposure to C_{60} as compared with IV exposure to C_{60}.

Post-I/R Serum Cytokines

The influence of IT or IV exposure to C_{60} on post-I/R concentrations of serum IL-6, MCP-1, and VEGF from male and female rats is presented in Figure 4(N = 3–4). IL-6 concentrations were greater in serum-collected post-I/R from male rats

TABLE 1
Physical Characterization of C_{60} and Vehicle Samples

	Hydrodynamic diameter (Z-average, nm) PDI and zeta values, mean ± SD								
	As-prepared sample (sample 1)			Sample 1 after 8 min			Sample 1 after 38 min		
	Z-average, nm	PDI	Zeta, mV	Z-average, nm	PDI	Zeta, mV	Z-average, nm	PDI	Zeta, mV
PVP	34.95 ± 1.91	1.0	−1.7	34.94 ± 1.97	ND	3.11	ND	ND	ND
PVP/C_{60}	371.3 ± 1.20	0.34 ± 0.02	1.78	371.3 ± 1.2	ND	1.78	369.6 ± 3.3	0.33 ± 0.01	1.5

ND, Not determined

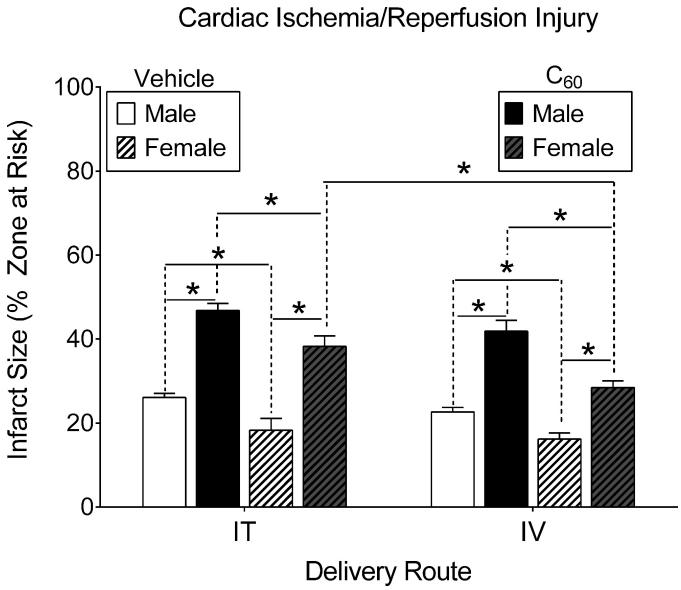

FIG. 3. Cardiac I/R injury. Male and female rats were subjected to regional cardiac I/R (20/120 min) injury *in situ*, 24 h following intratracheal (IT) or intravenous (IV) delivery of C_{60} or vehicle. In either case C_{60} exposure exacerbated myocardial infarction. Within each delivery route, infarct sizes in the male groups were larger than those in females. Between delivery routes, the females had larger infarctions in response to IT C_{60} exposure compared with IV exposure. *$p < 0.05$ by two-way ANOVA, $N = 4$–5.

exposed to IV C_{60} when compared with serum collected from male rats exposed to IV vehicle and male rats exposed to IT C_{60} (Fig. 4A). Female rats exposed to IV C_{60} had significantly lower serum IL-6 concentrations than IV C_{60} exposed males. Serum IL-6 concentrations were unaltered between all IT groups and IV exposed females. MCP-1 showed a similar profile to IL-6. MCP-1 concentrations were greater in serum-collected post-I/R from male rats exposed to C_{60} IV when compared with serum collected from male rats exposed to IV vehicle, male rats exposed to IT C_{60} and female rats exposed to C_{60} IV (Fig. 4B). Female rats exposed to IV C_{60} had significantly lower serum MCP-1 concentrations than IV C_{60} exposed males. Serum MCP-1 concentrations were unaltered between all IT groups and IV exposed females. VEGF was variable and slightly elevated in females exposed to IT and IV C_{60}, though not significantly different than any other group (Fig. 4C). Supplementary table 3 contains IL-6, MCP-1, VEGF, TNF-α, eotaxin, and IL-1β data from IV and IT exposed male rats for comparison of No-I/R and Post-I/R responses. In most cases the No-I/R groups demonstrated zero (below detection) to relatively low concentrations of cytokines 24 h postexposure.

Male Rat Coronary Artery Pharmacology

Pharmacological response curves generated in coronary artery (LAD) segments isolated from male rats 24 h after exposure to IT and IV administration of C_{60} or vehicle suspensions are shown in Figure 5($N = 4$–5). The associated EC_{50} and Hillslope values are reported in Table 3. LAD isolated from male rats exposed to IT C_{60} showed vascular smooth muscle stress (mN/mm^2) generation curves for 5-HT trending toward ($p = 0.06$) a leftward shift (i.e., sensitization) compared with the vehicle group (Fig. 5A). Stress response curves for 5-HT were not altered in LAD isolated from male rats treated with IV C_{60} or vehicle (Fig. 5B). ACh vascular smooth muscle relaxation responses were not different between LAD isolated from male rats exposed to IT C_{60} and vehicle (Fig. 5C). The LAD from IV C_{60} exposed males yielded an ACh vascular smooth muscle relaxation response curve with significantly different best-fit values than the curve generated by LAD isolated from vehicle exposed males, despite the overall variability ACh sensitivity (Fig. 5D). As indicated in Table 3, IT vehicle and IT C_{60} ACh EC_{50}s from male rats were significantly higher than those from naïve males. The ACh response curve produced by LAD from IV vehicle exposed males was not different from ACh responses in LAD isolated from naïve controls (curves not shown). Vascular smooth muscle relaxation curves generated by LAD in response to SNP were not different between IT exposed males (Fig. 5E) or IV exposed males (Fig. 5F). Curves from the naïve control group were not included in our graphed data in order to simplify presentation. We did include naïve male EC_{50} and Hillslope data in Table 3 in order to provide clarity in data interpretation and for purposes of discussion.

Female Rat Coronary Artery Pharmacology

Pharmacological response curves generated in coronary artery (LAD) segments isolated from female rats 24 h after ex-

TABLE 2
Rat Pulmonary Responses to Intratracheal (IT) or Intravenous (IV) Delivery of C_{60} or Vehicle Suspensions

	Total bronchoalveolar lavage fluid (BALF) protein and cellularity											
	BAL samples collected 24 h following exposure in males, data expressed as mean ± SEM											
	Protein (μg/ml)		Cell number ($\times 10^5$)		Macrophages ($\times 10^5$)		Neutrophils ($\times 10^3$)		Eosinophils ($\times 10^3$)		Epithelial cells ($\times 10^3$)	
	IT	IV	IT	IV	IT	IV	IT	IV	IT	IV	IT	IV
Vehicle	560 ± 149	638 ± 100	5.7 ± 1.4	3.5 ± 0.9	5.3 ± 1.3	5.7 ± 0.7	14.2 ± 10	2.1 ± 0.3	1.9 ± 1.1	2.4 ± 2.4	6.6 ± 2.4	1.7 ± 1.7
C_{60}	316 ± 55	750 ± 138*	3.9 ± 0.8	6.9 ± 1.7	4.0 ± 0.7	2.5 ± 1.2	13.3 ± 12	1.7 ± 1.4	0.5 ± 0.5	<1	2.8 ± 0.3	8.2 ± 2.6
Naïve	456 ± 31		5.6 ± 0.5		5.6 ± 0.5		7.7 ± 4.2		<1		8.7 ± 4.0	
n	4–5		4–6		3–5		3–5		3–5		3–5	

*$p < 0.05$ versus IT C_{60}.

	Total bronchoalveolar lavage fluid (BALF) protein and cellularity											
	BAL samples collected 24 h following exposure in females, data expressed as mean ± SEM											
	Protein (μg/ml)		Cell number ($\times 10^5$)		Macrophages ($\times 10^5$)		Neutrophils ($\times 10^3$)		Eosinophils ($\times 10^3$)		Epithelial cells ($\times 10^3$)	
	IT	IV	IT	IV	IT	IV	IT	IV	IT	IV	IT	IV
Vehicle	252 ± 28	195 ± 8.2	7.8 ± 1.9	4.1 ± 0.6†	1.6 ± 0.9	3.3 ± 0.4	35.0 ± 25.3	<1	0.25 ± 0.25*	1.7 ± 1.7	132 ± 90	346 ± 132
C_{60}	206 ± 24	226 ± 41	7.1 ± 1.2	3.5 ± 0.5*	0.9 ± 0.3	3.1 ± 1.1	27.5 ± 11.1	<1	12.5 ± 7.5	3.6 ± 0.6	75.0 ± 33	362 ± 59*
Naïve	N/A		6.6 ± 1.0		6.6 ± 1.1*,†		<1		<1		179 ± 43	
n	5–6		4–6		4–6		4–6		4–6		4–6	

N/A, not applicable.
*$p < 0.05$ versus IT C_{60}.
†$p < 0.05$ versus IT vehicle.

TABLE 3
Rat Coronary Artery Pharmacological Responses for Serotonin (5-HT), ACh, SNP, and ET-1

	Male rat EC_{50}s [nM] (mean ± SEM)						
	IT delivery			IV delivery			
	C_{60}	Vehicle	*p*-value, *n*	C_{60}	Vehicle	*p*-value, *n*	Naïve
5-HT	559 ± 104	871 ± 130	0.06, 4	766 ± 113	675 ± 59	0.25, 4	566 ± 130
ACh	265 ± 45*	239 ± 34*	0.33, 4	231 ± 80	97 ± 69	0.14, 4	123 ± 16
SNP	116 ± 24	76 ± 18	0.13, 4	76 ± 21	104 ± 53	0.32, 4	104 ± 25
ET-1	38 ± 20	48 ± 15	0.49, 6	26 ± 18	113 ± 86	0.35, 5	28 ± 8
	Male rat Hillslope values (mean ± SEM)						
	IT delivery			IV delivery			
	C_{60}	Vehicle	*p*-value, *n*	C_{60}	Vehicle	*p*-value, *n*	Naïve
5-HT	1.7 ± 0.1	3.2 ± 0.7	0.10, 4	2.0 ± 0.2	1.9 ± 0.1	0.57, 4	1.7 ± 0.2
ACh	2.6 ± 0.4	1.7 ± 0.1	0.10, 4	3.8 ± 0.8	1.8 ± 0.1	0.09, 3–4	1.8 ± 0.3
SNP	2.4 ± 0.6	2.2 ± 0.3	0.77, 4	2.1 ± 0.3	1.9 ± 0.1	0.50, 4	2.1 ± 0.4
ET-1	1.3 ± 0.2	1.0 ± 0.05*	0.09, 6	1.1 ± 0.1*	1.0 ± 0.2	0.67, 5	1.5 ± 0.1
	Female rat EC_{50}s [nM] (mean ± SEM)						
	IT delivery			IV delivery			
	C_{60}	Vehicle	*p*-value, *n*	C_{60}	Vehicle	*p*-value, *n*	
5-HT	813 ± 128	1268 ± 497	0.40, 5	932 ± 156	990 ± 275	0.86, 5	
ACh	1419 ± 843	139 ± 28	0.16, 5	619 ± 233	1085 ± 558	0.46, 5	
SNP	19 ± 3	21 ± 4	0.64, 5	14 ± 4	24.1 ± 4.1	0.16, 5	
ET-1	29 ± 20	6.5 ± 2.4	0.31, 5	13 ± 7	23 ± 16	0.56, 5	
	Female rat Hillslope values (mean ± SEM)						
	IT delivery			IV delivery			
	C_{60}	Vehicle	*p*-value, *n*	C_{60}	Vehicle	*p*-value, *n*	
5-HT	1.4 ± 0.4	1.0 ± 0.2	0.39, 5	1.3 ± 0.4	1.3 ± 0.2	0.95, 5	
ACh	1.0 ± 0.4	1.6 ± 0.3	0.29, 5	1.0 ± 0.2	1.7 ± 0.5	0.19, 5	
SNP	1.6 ± 0.3	2.1 ± 0.4	0.35, 4	2.0 ± 0.3	1.9 ± 0.3	0.79, 5	
ET-1	1.4 ± 0.3	1.1 ± 0.3	0.41, 5	1.1 ± 0.2	1.0 ± 0.2	0.67, 5	

*$p < 0.05$ versus Naïve.

posure to IT and IV administration of C_{60} or vehicle suspensions are shown in Figure 6($N = 5$). The associated EC_{50} and Hillslope values are also reported in Table 3. Stress generation curves for 5-HT were not significantly different between LAD isolated from female rats exposed to IT C_{60} or vehicle (Fig. 6A). LAD vascular smooth muscle stress generation in response to 5-HT was not different between LAD from the female IV C_{60} or IV vehicle groups (Fig. 6B). Vascular smooth muscle relaxation in response to ACh was not different between LAD isolated from female rats exposed to IT C_{60} or IT vehicle (Fig. 6C). The vascular smooth muscle relaxation response curves for ACh appeared to show a desensitization in the LAD from IV C_{60} exposed females, but the responses were not statistically different from females exposed to IV vehicle (Fig. 6D). The best-fit values for the vascular smooth muscle relaxation curve for SNP in IT C60 exposed females were significantly different than those from IT vehicle exposed females (Fig. 6E) and IV exposed males (Fig. 6F).

Coronary Responses to ET-1

Vascular smooth muscle contraction responses to ET-1 in LAD segments isolated from male and female rats exposed to IT or IV C_{60} and vehicle are shown in Figure 7($N = 5$). Coronary artery segments isolated from male rats exposed to IT C_{60} showed increased stress generation in response to ET-1 than coronary artery segments isolated from male rats exposed to IT vehicle (Fig. 7A). Coronary artery segments isolated from male rats exposed IV to C_{60} or vehicle were not different between groups (Fig. 7B). ET-1 responses in coronary artery segments isolated from female rats were not different between C60 or vehicle by IT instillation (Fig. 7C) or IV instillation (Fig. 7D). EC_{50} and Hillslope values for ET-1 concentration-response curves are reported in Table 3 for LAD collected from naïve, IT vehicle and IT C_{60} exposed rats.

Indomethacin-Sensitive Coronary Artery Responses to ET-1

The ability of Indomethacin to influence ET-1 mediated isometric stress (mN/mm^2) generation in LAD isolated from male rats exposed to IT C_{60} is depicted in Figure 8($N = 6$). LAD seg-

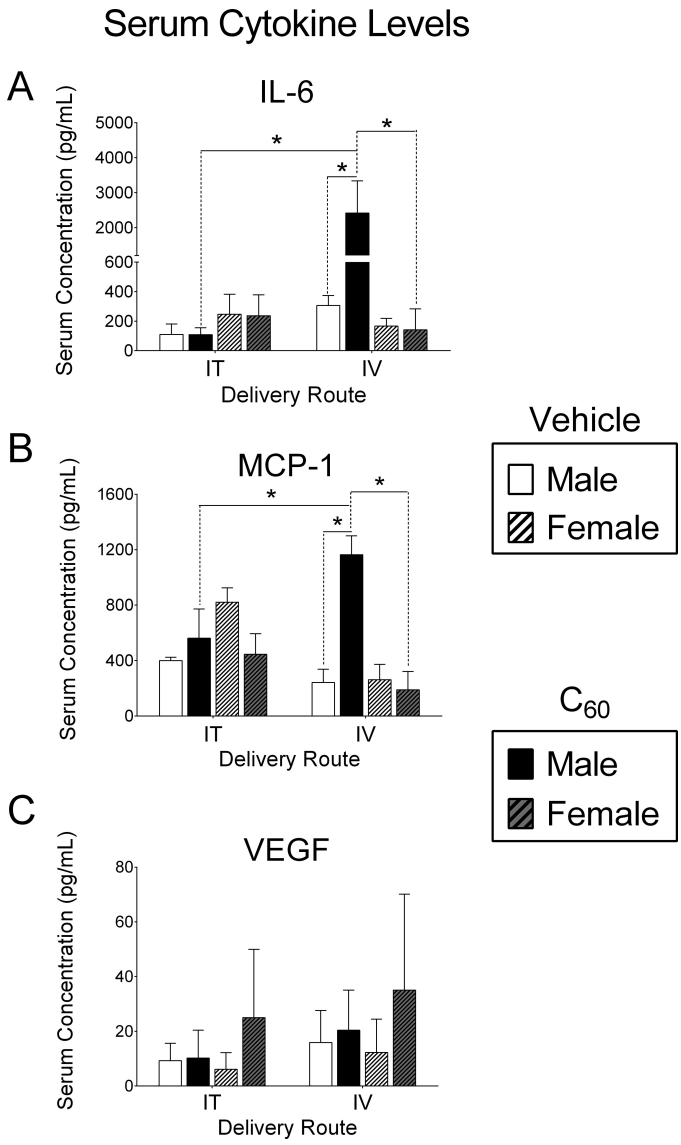

FIG. 4. Post-I/R injury serum cytokine concentrations. Serum samples were collected from male or female rats subjected to cardiac I/R injury, 24 h following intratracheal (IT) or intravenous (IV) delivery of C_{60} or vehicle. (A) IL-6 concentrations were significantly higher in serum collected from male rats exposed to IV C_{60} compared with male IV vehicle, male IT C_{60}, and female IV C_{60}. (B) MCP-1 concentrations were also increased in serum collected from male rats exposed to IV C_{60} compared with male IV vehicle, male IT C_{60}, and female IV C_{60}. (C) VEGF concentrations were similar in serum collected from all groups. $*p < 0.05$ by two-way ANOVA, $N = 3–4$.

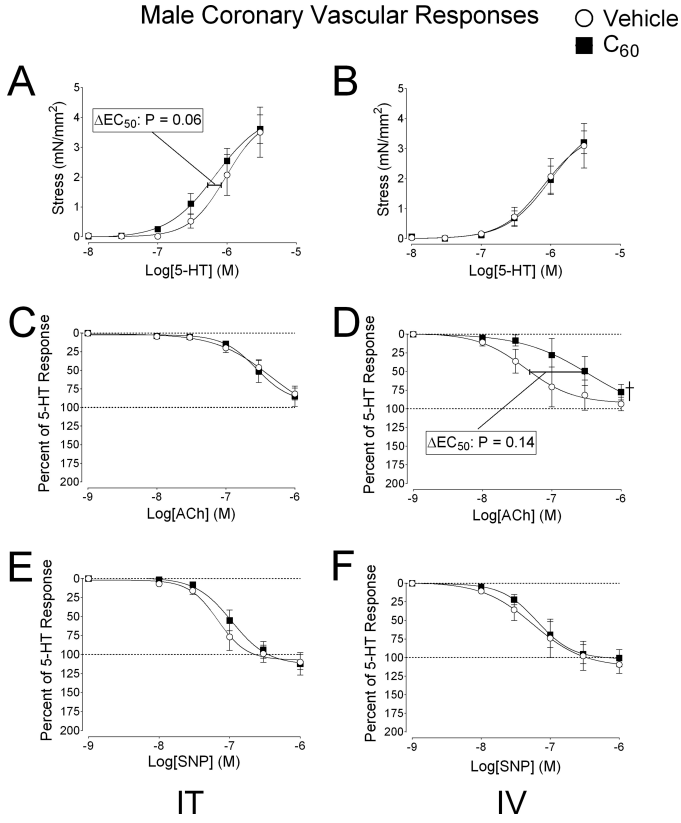

FIG. 5. Experimental coronary artery pharmacology in male rats. Segments of the coronary artery (LAD) were isolated from male rats 24 h following intratracheal (IT) or intravenous (IV) delivery of C_{60} or vehicle. (A) Cumulative concentration-response curves for serotonin (5-HT) revealed a trend for sensitized vascular smooth muscle contraction in coronary arteries from IT C_{60} exposed rats, which were not seen following IV delivery of C_{60}. (B) Cumulative concentration-response curves for 5-HT in coronary artery smooth muscle of LAD segments isolated from IV exposed rats. (C) Cumulative concentration-response curves for ACh showed no changes following IT exposure. (D) The IV C_{60} ACh curve was rightward shifted compared with the vehicle curve. (E) Cumulative concentration-response curves for SNP were similar between vehicle and C_{60} groups following IT exposure and IV exposure. (F) Cumulative SNP concentration-response curves from LAD isolated from IV exposed rats. $\dagger p < 0.05$ by regression analysis of best-fit curve values. Reported p-values for ΔEC_{50} were determined by t-test, $N = 4–5$.

ments isolated from rats exposed to C_{60} generated more stress in response to ET-1 than LAD collected from vehicle exposed rats (Fig. 8A). Enhanced stress was lower in paired LAD isolated from C_{60} exposed rats that were incubated with 10μM Indomethacin, a general COX inhibitor, for 20 min immediately prior to ET-1 protocols (Fig. 8B). LAD collected from vehicle instilled rats did not show sensitivity to Indomethacin inhibition of COX during ET-1 mediated vascular smooth muscle contraction, but Indomethacin inhibition was able to restore the C_{60} stress generation response to ET-1 to the level of the vehicle group (Fig. 8C).

DISCUSSION

This study demonstrated that IT C_{60} exposure of Sprague Dawley rats resulted in deleterious cardiovascular consequences. This included C_{60}-induced expansion of myocardial infarction following cardiac I/R and enhancement of ET-1 mediated stress generation of isolated segments of the LAD, potentially indicative of increased coronary vascular resistance.

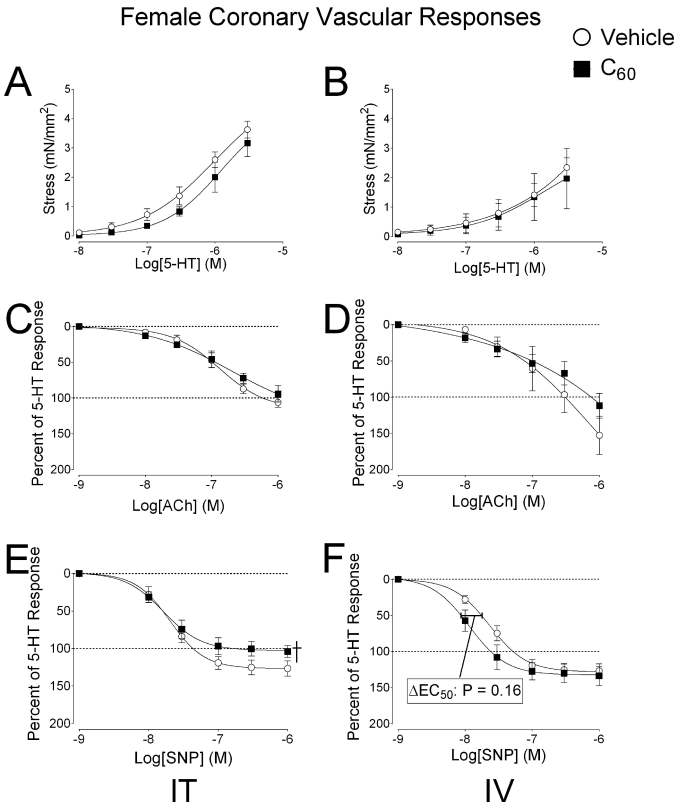

FIG. 6. Experimental coronary artery pharmacology in female rats. Segments of the coronary artery (LAD) were isolated from female rats 24 h following intratracheal (IT) or intravenous (IV) delivery of C_{60} or vehicle. (A) Cumulative concentration-response curves for serotonin (5-HT) mediated vascular smooth muscle contraction in LAD from IT C_{60} exposed rats. (B) Cumulative concentration-response curves for 5-HT in coronary artery smooth muscle of LAD segments isolated from IV exposed rats. (C) Cumulative concentration-response curves for ACh showed no changes following IT exposure. (D) The IV C_{60} ACh curve a slight rightward shifted compared with the vehicle curve. (E) Cumulative concentration-response curves for SNP showed less smooth muscle relaxation in LAD isolated from IT C_{60} compared with IT vehicle groups. (F) Cumulative SNP concentration-response curves from LAD isolated from IV exposed rats showed slight leftward shifts in EC_{50} from LAD coronary artery smooth muscle relaxation responses from C_{60} exposed females compared with the IV vehicle curves. †$p < 0.05$ by regression analysis of best-fit curve values. Reported p-values for ΔEC_{50} were determined by t-test, $N = 4$–5.

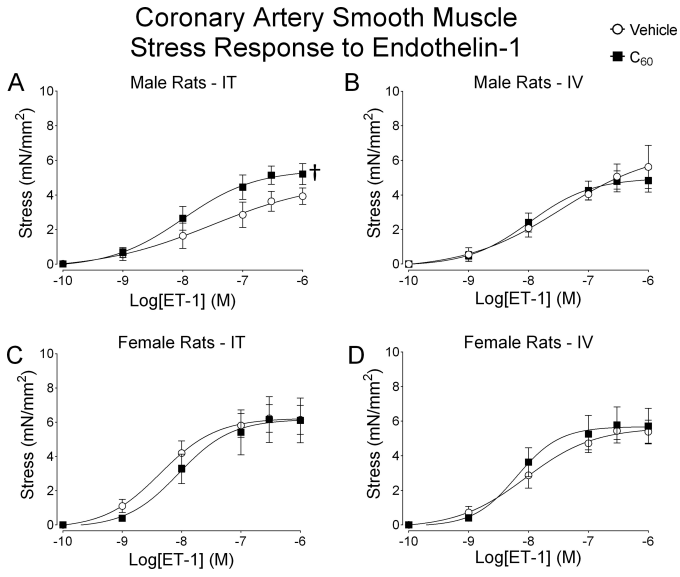

FIG. 7. Male and female coronary artery responses to ET-1. Segments of the coronary artery were isolated from male and female rats 24 h following IT or IV delivery of C_{60} or vehicle. (A) Cumulative concentration-response curves for ET-1 showed enhanced stress generation during isometric vascular smooth muscle contraction in LAD from IT C_{60} instilled male rats compared with vehicle. (B) Cumulative concentration-response curves for ET-1 stress generation during isometric vascular smooth muscle contraction in LAD from IV C_{60} or vehicle instilled male rats. (C) Cumulative concentration-response curves for ET-1 stress generation during isometric vascular smooth muscle contraction in LAD from IT C_{60} instilled female rats. (D) Cumulative concentration-response curves for ET-1 stress generation during isometric vascular smooth muscle contraction in LAD from IV C_{60} instilled female rats. †$p < 0.05$ by regression analysis of best-fit curve values. $N = 5$–6.

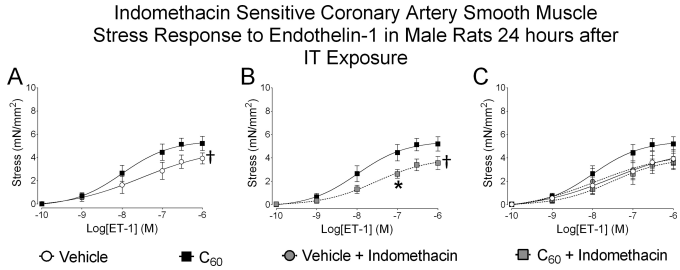

FIG. 8. Indomethacin-sensitive coronary artery responses to ET-1. Segments of the coronary artery were isolated from male rats 24 h following IT delivery of C_{60} or vehicle. Paired LAD segments isolated from each of the IT exposed male rats were also treated with 10μM Indomethacin 20 min prior to ET-1 administration. (A) Cumulative concentration-response curves developed in response to ET-1 revealed enhanced isometric stress generation in coronary arteries from C_{60} exposed rats when compared with vehicle. (B) Coronary segments isolated from C_{60} exposed rats showed sensitivity to Indomethacin during cumulative concentration responses to ET-1 when compared with vehicle. (C) Data combined from vehicle and C_{60} groups during ET-1/Indomethacin experiments showed that LAD isolated from vehicle instilled rats was not sensitive to Indomethacin during cumulative concentration responses to ET-1 and that Indomethacin restored LAD smooth muscle contractile response from IT C_{60} exposed rats to the level of those from the vehicle group. †$p < 0.05$ by regression analysis of best-fit curve values, *$p < 0.05$ by repeated measures ANOVA on matching concentration data points, $N = 6$.

These results align with the paradigm that pulmonary exposure to nanosized particles has the potential to generate cardiovascular impairments (Brook *et al.*, 2010; Mann *et al.*, 2012; Mills *et al.*, 2009; Shannahan *et al.*, 2012) and supports our previous report that enhanced coronary artery tone following IT exposure to engineered carbon nanomaterials may exacerbate cardiac I/R injury (Thompson *et al.*, 2012). The present study goes further to demonstrate that IT exposure to C_{60} may generate cardiovascular detriments via mechanisms unique from those produced by IV exposure to C_{60}. Although expansion of post-I/R myocardial infarction resulted from both IT and IV exposure to C_{60}, our study uncovered impairment of ACh mediated coronary artery relaxation, increased serum IL-6 and serum MCP-1 associated

with IV C_{60} exposure and not IT C_{60} exposure in male rats. This study also offers other evidence of potential importance in that female rats were more susceptible to I/R injury following IT C_{60} exposure than they were following IV C_{60} exposure, a trend that did not emerge in male rats. Female rats also showed sensitivity to C_{60} exposure route by coronary artery relaxation response to SNP. The diminished SNP response in the female IT C_{60} group was not seen in the female IV C_{60} group. The female IT C60 group also had significant eosinophilia when compared with the IT vehicle female group. These findings provide a possible explanation for why infarct sizes were larger in the female IT C_{60} group than infarcts in the female IV C_{60} group. These types of gender sensitivities to nanomaterials are not well understood and may be an important area for future research.

C_{60} fullerene is emerging as an advantageous engineered nanoparticle due to its highly modifiable structure, potentially providing it with countless applications in material science (Min *et al.*, 2012), optics, cosmetics (Turco *et al.*, 2011), electronics, green energy (Morinaka *et al.*, 2013), and medicine (Fan *et al.*, 2013). With C_{60} use increasing, the toxicological and regulatory communities have been investigating the potential adverse impacts associated with C_{60} exposure, bringing into question potential routes of exposure and use of comparable doses. Pulmonary exposure is expected to occur in occupations requiring direct work with raw C_{60}. In occupational settings C_{60} have been detected at concentrations ranging from 23,856 to 53,119 particles/L air (Johnson *et al.*, 2010). Considering that humans breathe between 360 and 600 L of air an hour, even a brief 1 h occupational inhalation exposure could deposit 8,500,000–31,500,00 C_{60} particles into the lungs. We delivered 515,825 $\pm$ 27,014 C_{60} particles to each rat in the C_{60} groups from our study. Given the size difference between rats and humans, the 28 μg C_{60} burden we administered to each rat was relatively large, but comparable to potential human doses.

Studies have shown that IT instillation of 100 μg C_{60} in rats resulted in a pulmonary burden half-life of about 15 days (Shinohara *et al.*, 2010) and minimal pulmonary inflammation 3 days after exposure (Ogami *et al.*, 2011). The medical applications of C_{60} suggest that IV exposure in humans is likely. In a study where C_{60} was administered IV to male rats once per day for 4 days ($\sim$929 μg C_{60} total), C_{60} accumulation in the lungs was prominent from 1 day postexposure out to 28 days postexposure (Kubota *et al.*, 2011). Another IV study on the biodistribution of radiolabeled C_{60} in pregnant and lactating rats showed moderate accumulation of C_{60} in the lungs (Sumner *et al.*, 2010). The cytotoxicity of unmodified C_{60} has been examined *in vitro* and several reports agree that cytotoxicity is minimal to moderate, if any (Jia *et al.*, 2005; Kovochich *et al.*, 2009; Shinohara *et al.*, 2009; Song *et al.*, 2012). We delivered 28 μg of C_{60} per rat in this study (93.33 μg/kg based on a 300 g rat) and 0.1–10 $\mu g/cm^2$ in our *in vitro* experiments, doses comparable and often times lower than the doses of other C_{60} studies cited. Though we found an increase in eosinophils in the female IT C_{60} group compared with IT vehicle, our study falls in line with many of those studies supporting the possibility that C_{60} delivered IT or IV may produce minimal pulmonary inflammation or direct cytotoxicity, if any.

Despite the various investigations into pulmonary and *in vitro* responses to C_{60}, examinations of cardiovascular impacts are scarce. The model of *in situ* cardiac I/R injury used in this study has been well established in our laboratory as a toxicological endpoint following pulmonary exposure to various types of ultrafine and nanosized particles (Cozzi *et al.*, 2006; Katwa *et al.*, 2012; Urankar *et al.*, 2012). Here we tested the hypothesis that pulmonary exposure to C_{60} would result in expansion of myocardial infarction in rats subjected to cardiac I/R injury 24 h postexposure. Our results maintain that IT exposure to nanoparticles exacerbates myocardial infarction in a male rat model. We further tested the possibility that the route of exposure may uniquely alter the I/R injury between IT and IV exposure to C_{60}. This did not appear to be the case in male rats as shown in Figure 7. However, the extent of post-I/R myocardial infarction in female rats was significantly larger in the IT C_{60} exposed group compared with the IV C_{60} exposed group, suggesting that gender may influence the biological response to C_{60} exposure.

Though post-I/R myocardial infarct sizes were not greatly different between IT and IV C_{60} exposed males, serum IL-6 and MCP-1 concentrations were significantly elevated post-I/R in the IV C_{60} group compared with the IT C_{60} group. It is unclear if these elevated serum components found after cardiac I/R contributed to the infarct expansion or were merely a reflection of the infarct size. Further, it is unclear as to why male rats produced an IL-6/MCP-1 response following I/R in the IV C_{60} group but the female group did not. We can speculate that perhaps a link between cardioprotection and estrogen may also contribute to reduced IL-6 and MCP-1 release in response to cardiac I/R. In any case, IL-6 and MCP-1 have each been linked to impaired fibrinolysis/hemostasis following exposure to particulate matter (Budinger *et al.*, 2011; Emmerechts *et al.*, 2010), which can promote thrombi-dependent zones of no reflow in the myocardium during I/R and exacerbate infarction. IL-6 is associated with acute myocardial infarction (Anderson *et al.*, 2013) and promotes the release of C-reactive protein, an acute-phase protein linked to myocardial infarction and increased production of MCP-1 (Schuett *et al.*, 2009). MCP-1 is involved in neutrophil and macrophage recruitment into the myocardial risk area following I/R, and the release of MCP-1 following I/R injury has been implicated in diminished vagal nerve activity (Calvillo *et al.*, 2011). Given the MCP-1 concentrations reported herein and the report that ultrafine carbon particle exposure depresses vagal tone (Harder *et al.*, 2005), the assessment of vagal tone following C_{60} exposure may be important in future studies.

We also examined pharmacological responsiveness of isolated LAD in order to link C_{60} exposure to enhanced coronary artery tone. Vascular tone is an important physiological determinant of tissue perfusion and blood flow by impacting artery diameter and vascular resistance. As vascular tone increases,

vessel diameter decreases and thus perfusion flow decreases (Badeer, 2001). Coronary perfusion of the myocardial zone at risk for infarction during I/R can occur by collateral flow during ischemia and reflow during reperfusion. Enhanced coronary arterial tone due to particle exposure could impair collateral flow during ischemia and promote zones of no reflow during reperfusion. The LAD from IT C_{60} exposed male rats did show a trend for sensitized 5-HT mediated vascular smooth muscle contraction in our initial assessment of a vascular contribution to the cardiac I/R injury following IT exposure to C_{60}. Those LAD experiments also indicated that IV C_{60} exposure may have impacted vascular tone uniquely from IT exposure to C_{60} by promoting impaired ACh endothelium-dependent vascular smooth muscle relaxation in the LAD. Unexpectedly, these experiments indicated that in male rats, LAD from the IT vehicle group had diminished ACh responsiveness when compared with the naïve group. In female rats, 5-HT responsiveness and ACh responses were only minimally altered, but a rightward shift in the LAD relaxation response to ACh in the IV C_{60} group was noticeable. The larger changes in the pharmacological assessments of female LAD came in the SNP concentration-response studies, in which the route of exposure seemed to play a role. In these experiments, the female IT C_{60} group had diminished responsiveness to the NO donor SNP. This response was not recapitulated in the female IV C_{60} group and the response also offers a possible explanation for why the female IT C_{60} group had larger I/R infarct sizes than the IV C_{60} group.

It is possible that slight shifts toward enhanced vascular tone during pharmacological assessments of LAD segments may function as an indicator of more robust vascular tone in the greater coronary circulation, especially during a period of cardiac reperfusion following an ischemic bout. We have previously reported that one day after IT exposure to multi-walled carbon nanotubes in rats, isolated LAD segments generated slightly more stress in response to ET-1 but coronary flow was significantly depressed during postischemic reperfusion of isolated Langendorff rat hearts (Thompson *et al.*, 2012). Those enhanced isolated LAD ET-1 responses appeared to be associated with the COX pathway, a physiological response mechanism documented in various vascular beds following pulmonary exposure to nanoparticles (Cuevas *et al.*, 2010; Knuckles *et al.*, 2012; LeBlanc *et al.*, 2010). These reports prompted us to examine COX-dependent ET-1 stress responses in isolated LAD from rats exposed to IT C_{60} and vehicle. Maximal stress responses to ET-1 were more pronounced in the IT C_{60} exposed group compared with the IT vehicle group. Inhibition with 10μM Indomethacin, a general COX inhibitor, prevented the increased LAD stress in response to ET-1 seen in the IT C_{60} group and had no effect in LAD from IT vehicle exposed rats. These data support our hypothesis that enhanced coronary tone may have contributed to exacerbation of post-I/R myocardial infarction we found in the IT C_{60} exposed rats as compared with the IT vehicle exposed rats.

The findings in this study provide support that the cardiovascular system as a whole is susceptible to nanoparticle exposure, especially at the pulmonary interface. Although the entire set of mechanisms that contribute to exacerbation of I/R infarction are unclear, the vascular system appears to contribute to the deleterious cardiovascular consequences of nanoparticle exposure. The arterial system must maintain appropriate sensitivity to stimuli present in the immediate extracellular environment in order to adequately respond to the perfusion needs of the tissue and organ. If the arterial system loses its ability to respond to stimuli appropriately, the homeostatic window for organ perfusion may narrow and may leave the tissue/organ susceptible to injury should an insult arise. It appears from our data reported here, and in previous work (Thompson *et al.*, 2012), that 24 h following nanoparticle exposure, pharmacological responsiveness to chemical ligands may be disrupted in coronary arteries. Our findings of coronary dysfunction following nanoparticle exposure are also consistent with other investigations into coronary endpoints following nanoparticle exposure (LeBlanc *et al.*, 2010; Minarchick *et al.*, 2013; Stapleton *et al.*, 2012). Such changes in coronary artery physiology can have serious detrimental health effects, especially during an ischemic emergency.

We conclude that the heart is susceptible to I/R injury 24 h following IT or IV exposure to C_{60} despite minimal pulmonary inflammation and little evidence that C_{60} is cytotoxic *in vitro*. Novel to our initial predictions, administration of IV C_{60} also promoted infarct expansion following cardiac I/R 24 h postexposure and we offer evidence that the mechanisms that drive that injury may be unique from IT exposure. These mechanisms include differential impacts on the coronary vasculature that promote enhanced coronary tone. These ranged from enhanced ET-1 stress generation to depressed ACh responsiveness. Additionally, there may be some gender sensitivity to C_{60} administration routes. IV exposure to C_{60} may uniquely modulate cytokine release during cardiac I/R. We further caution that the choice of vehicles and dispersants used may have unexpected biological influences. Because C_{60} applications are growing in industry and medicine, awareness of potential cardiovascular consequences of exposure may improve safety regulations, broaden the medical uses of C_{60} through directed toxicity, and improve physicochemical modifications of C_{60}.

SUPPLEMENTARY DATA

Supplementary data are available online at http://toxsci.oxfordjournals.org/.

FUNDING

National Institute of Environmental Health Sciences [U19 ES019525]; East Carolina University and RTI International.

ACKNOWLEDGMENTS

We would like to thank Louise D. Mayer for preparing the carbon-14 uniformly labeled C_{60}; Catherine O'Sullivan who prepared all the vials of C_{60}/PVP and PVP vehicle samples; Jillian Odom, Erin Mann, and Daniel Becak for assistance with isolated coronary artery data collection and bronchoalveolar lavage fluid collection/analysis.

REFERENCES

Anderson, D. R., Poterucha, J. T., Mikuls, T. R., Duryee, M. J., Garvin, R. P., Klassen, L. W., Shurmur, S. W., and Thiele, G. M. (2013). IL-6 and its receptors in coronary artery disease and acute myocardial infarction. *Cytokine* **62**, 395–400.

Badeer, H. S. (2001). Hemodynamics for medical students. *Adv. Physiol. Educ.* **25**, 44–52.

Baker, G. L., Gupta, A., Clark, M. L., Valenzuela, B. R., Staska, L. M., Harbo, S. J., Pierce, J. T., and Dill, J. A. (2008). Inhalation toxicity and lung toxicokinetics of C60 fullerene nanoparticles and microparticles. *Toxicol. Sci.* **101**, 122–131.

Bakry, R., Vallant, R. M., Najam-ul-Haq, M., Rainer, M., Szabo, Z., Huck, C. W., and Bonn, G. K. (2007). Medicinal applications of fullerenes. *Int. J. Nanomed.* **2**, 639–649.

Brook, R. D., Rajagopalan, S., Pope, C. A., III, Brook, J. R., Bhatnagar, A., ez-Roux, A. V., Holguin, F., Hong, Y., Luepker, R. V., Mittleman, M. A., *et al.* (2010). Particulate matter air pollution and cardiovascular disease: An update to the scientific statement from the American Heart Association. *Circulation* **121**, 2331–2378.

Budinger, G. R., McKell, J. L., Urich, D., Foiles, N., Weiss, I., Chiarella, S. E., Gonzalez, A., Soberanes, S., Ghio, A. J., Nigdelioglu, R., *et al.* (2011). Particulate matter-induced lung inflammation increases systemic levels of PAI-1 and activates coagulation through distinct mechanisms. *PLoS One* **6**, e18525.

Bunz, H., Plankenhorn, S., and Klein, R. (2012). Effect of buckminsterfullerenes on cells of the innate and adaptive immune system: An in vitro study with human peripheral blood mononuclear cells. *Int. J. Nanomed.* **7**, 4571–4580.

Calvillo, L., Vanoli, E., Andreoli, E., Besana, A., Omodeo, E., Gnecchi, M., Zerbi, P., Vago, G., Busca, G., and Schwartz, P. J. (2011). Vagal stimulation, through its nicotinic action, limits infarct size and the inflammatory response to myocardial ischemia and reperfusion. *J. Cardiovasc. Pharmacol.* **58**, 500–507.

Campen, M. J., Lund, A., and Rosenfeld, M. (2012). Mechanisms linking traffic-related air pollution and atherosclerosis. *Curr. Opin. Pulm. Med.* **18**, 155–160.

Cozzi, E., Hazarika, S., Stallings, H. W., III, Cascio, W. E., Devlin, R. B., Lust, R. M., Wingard, C. J., and Van Scott, M. R. (2006). Ultrafine particulate matter exposure augments ischemia-reperfusion injury in mice. *Am. J. Physiol. Heart Circ. Physiol.* **291**, H894–H903.

Cuevas, A. K., Liberda, E. N., Gillespie, P. A., Allina, J., and Chen, L. C. (2010). Inhaled nickel nanoparticles alter vascular reactivity in C57BL/6 mice. *Inhal. Toxicol.* **22**(Suppl. 2), 100–106.

Delfino, R. J., Sioutas, C., and Malik, S. (2005). Potential role of ultrafine particles in associations between airborne particle mass and cardiovascular health. *Environ. Health Perspect.* **113**, 934–946.

Du, Z., Zhao, D., Jing, L., Cui, G., Jin, M., Li, Y., Liu, X., Liu, Y., Du, H., Guo, C., *et al.* (2013). Cardiovascular Toxicity of Different Sizes Amorphous Silica Nanoparticles in Rats After Intratracheal Instillation. *Cardiovasc. Toxicol.* **13**, 194–207.

Emmerechts, J., Alfaro-Moreno, E., Vanaudenaerde, B. M., Nemery, B., and Hoylaerts, M. F. (2010). Short-term exposure to particulate matter induces arterial but not venous thrombosis in healthy mice. *J. Thromb. Haemost.* **8**, 2651–2661.

Fan, J., Fang, G., Zeng, F., Wang, X., and Wu, S. (2013). Water-dispersible fullerene aggregates as a targeted anticancer prodrug with both chemo- and photodynamic therapeutic actions. *Small* **9**, 613–621.

Gustafsson, A., Lindstedt, E., Elfsmark, L. S., and Bucht, A. (2011). Lung exposure of titanium dioxide nanoparticles induces innate immune activation and long-lasting lymphocyte response in the Dark Agouti rat. *J. Immunotoxicol.* **8**, 111–121.

Halpern, W., and Mulvany, M. J. (1977). Tension responses to small length changes of vascular smooth muscle cells [proceedings]. *J. Physiol.* **265**, 21P-23P.

Harder, V., Gilmour, P., Lentner, B., Karg, E., Takenaka, S., Ziesenis, A., Stampfl, A., Kodavanti, U., Heyder, J., and Schulz, H. (2005). Cardiovascular responses in unrestrained WKY rats to inhaled ultrafine carbon particles. *Inhal. Toxicol.* **17**, 29–42.

Jia, G., Wang, H., Yan, L., Wang, X., Pei, R., Yan, T., Zhao, Y., and Guo, X. (2005). Cytotoxicity of carbon nanomaterials: Single-wall nanotube, multi-wall nanotube, and fullerene. *Environ. Sci. Technol.* **39**, 1378–1383.

Johnson, D. R., Methner, M. M., Kennedy, A. J., and Steevens, J. A. (2010). Potential for occupational exposure to engineered carbon-based nanomaterials in environmental laboratory studies. *Environ. Health Perspect.* **118**, 49–54.

Katwa, P., Wang, X., Urankar, R. N., Podila, R., Hilderbrand, S. C., Fick, R. B., Rao, A. M., Ke, P. C., Wingard, C. J., and Brown, J. M. (2012). A carbon nanotube toxicity paradigm driven by mast cells and the IL-(3)(3)/ST(2) axis. *Small* **8**, 2904–2912.

Knuckles, T. L., Yi, J., Frazer, D. G., Leonard, H. D., Chen, B. T., Castranova, V., and Nurkiewicz, T. R. (2012). Nanoparticle inhalation alters systemic arteriolar vasoreactivity through sympathetic and cyclooxygenase-mediated pathways. *Nanotoxicology* **6**, 724–735.

Kovochich, M., Espinasse, B., Auffan, M., Hotze, E. M., Wessel, L., Xia, T., Nel, A. E., and Wiesner, M. R. (2009). Comparative toxicity of C60 aggregates toward mammalian cells: Role of tetrahydrofuran (THF) decomposition. *Environ. Sci. Technol.* **43**, 6378–6384.

Kubota, R., Tahara, M., Shimizu, K., Sugimoto, N., Hirose, A., and Nishimura, T. (2011). Time-dependent variation in the biodistribution of C(6)(0) in rats determined by liquid chromatography-tandem mass spectrometry. *Toxicol. Lett.* **206**, 172–177.

LeBlanc, A. J., Moseley, A. M., Chen, B. T., Frazer, D., Castranova, V., and Nurkiewicz, T. R. (2010). Nanoparticle inhalation impairs coronary microvascular reactivity via a local reactive oxygen species-dependent mechanism. *Cardiovasc. Toxicol.* **10**, 27–36.

Ludbrook, J. (1994). Repeated measurements and multiple comparisons in cardiovascular research. *Cardiovasc. Res.* **28**, 303–311.

Mann, E. E., Thompson, L. C., Shannahan, J. H., and Wingard, C. J. (2012). Changes in cardiopulmonary function induced by nanoparticles. *Wiley Interdiscip. Rev. Nanomed. Nanobiotechnol.* **4**, 691–702.

Mills, N. L., Donaldson, K., Hadoke, P. W., Boon, N. A., MacNee, W., Cassee, F. R., Sandstrom, T., Blomberg, A., and Newby, D. E. (2009). Adverse cardiovascular effects of air pollution. *Nat. Clin. Pract. Cardiovasc. Med.* **6**, 36–44.

Min, J., Shah, P. N., Chae, C. G., and Lee, J. S. (2012). Arrangement of C60 via the self-assembly of post-functionalizable polyisocyanate block copolymer. *Macromol. Rapid Commun.* **33**, 2029–2034.

Minarchick, V. C., Stapleton, P. A., Porter, D. W., Wolfarth, M. G., Ciftyurek, E., Barger, M., Sabolsky, E. M., and Nurkiewicz, T. R. (2013). Pulmonary cerium dioxide nanoparticle exposure differentially impairs coronary and mesenteric arteriolar reactivity. *Cardiovasc. Toxicol.* **13**, 323–337.

Morimoto, Y., Hirohashi, M., Ogami, A., Oyabu, T., Myojo, T., Nishi, K., Kadoya, C., Todoroki, M., Yamamoto, M., Murakami, M., *et al.* (2010). In-

flammogenic effect of well-characterized fullerenes in inhalation and intratracheal instillation studies. *Part. Fibre Toxicol.* **7**, 4.

Morinaka, Y., Nobori, M., Murata, M., Wakamiya, A., Sagawa, T., Yoshikawa, S., and Murata, Y. (2013). Synthesis and photovoltaic properties of acceptor materials based on the dimerization of fullerene C60 for use in efficient polymer solar cells. *Chem. Commun. (Camb.)* **49**, 3670–3672.

Ogami, A., Yamamoto, K., Morimoto, Y., Fujita, K., Hirohashi, M., Oyabu, T., Myojo, T., Nishi, K., Kadoya, C., Todoroki, M., *et al.* (2011). Pathological features of rat lung following inhalation and intratracheal instillation of C(60) fullerene. *Inhal. Toxicol.* **23**, 407–416.

Park, E. J., Kim, H., Kim, Y., Yi, J., Choi, K., and Park, K. (2010). Inflammatory responses may be induced by a single intratracheal instillation of iron nanoparticles in mice. *Toxicology* **275**, 65–71.

Schuett, H., Luchtefeld, M., Grothusen, C., Grote, K., and Schieffer, B. (2009). How much is too much? Interleukin-6 and its signalling in atherosclerosis. *Thromb. Haemost.* **102**, 215–222.

Shannahan, J. H., Kodavanti, U. P., and Brown, J. M. (2012). Manufactured and airborne nanoparticle cardiopulmonary interactions: A review of mechanisms and the possible contribution of mast cells. *Inhal. Toxicol.* **24**, 320–339.

Shinohara, N., Gamo, M., and Nakanishi, J. (2011). Fullerene c60: Inhalation hazard assessment and derivation of a period-limited acceptable exposure level. *Toxicol. Sci.* **123**, 576–589.

Shinohara, N., Matsumoto, K., Endoh, S., Maru, J., and Nakanishi, J. (2009). In vitro and in vivo genotoxicity tests on fullerene C60 nanoparticles. *Toxicol. Lett.* **191**, 289–296.

Shinohara, N., Nakazato, T., Tamura, M., Endoh, S., Fukui, H., Morimoto, Y., Myojo, T., Shimada, M., Yamamoto, K., Tao, H., *et al.* (2010). Clearance kinetics of fullerene C(6)(0) nanoparticles from rat lungs after intratracheal C(6)(0) instillation and inhalation C(6)(0) exposure. *Toxicol. Sci.* **118**, 564–573.

Song, M., Yuan, S., Yin, J., Wang, X., Meng, Z., Wang, H., and Jiang, G. (2012). Size-dependent toxicity of nano-C60 aggregates: More sensitive indication by apoptosis-related Bax translocation in cultured human cells. *Environ. Sci. Technol.* **46**, 3457–3464.

Stapleton, P. A., Minarchick, V. C., Cumpston, A. M., McKinney, W., Chen, B. T., Sager, T. M., Frazer, D. G., Mercer, R. R., Scabilloni, J., Andrew, M. E., *et al.* (2012). Impairment of coronary arteriolar endothelium-dependent dilation after multi-walled carbon nanotube inhalation: A time-course study. *Int. J. Mol. Sci.* **13**, 13781–13803.

Sumner, S. C., Fennell, T. R., Snyder, R. W., Taylor, G. F., and Lewin, A. H. (2010). Distribution of carbon-14 labeled C60 ([14C]C60) in the pregnant and in the lactating dam and the effect of C60 exposure on the biochemical profile of urine. *J. Appl. Toxicol.* **30**, 354–360.

Tawfik, H. E., Cena, J., Schulz, R., and Kaufman, S. (2008). Role of oxidative stress in multiparity-induced endothelial dysfunction. *Am. J. Physiol. Heart Circ. Physiol.* **295**, H1736–H1742.

Thompson, L. C., Frasier, C. R., Sloan, R. C., Mann, E. E., Harrison, B. S., Brown, J. M., Brown, D. A., and Wingard, C. J. (2014). Pulmonary instillation of multi-walled carbon nanotubes promotes coronary vasoconstriction and exacerbates injury in isolated hearts. *Nanotoxicology.* **8**, 38–49.

Turco, R. F., Bischoff, M., Tong, Z. H., and Nies, L. (2011). Environmental implications of nanomaterials: Are we studying the right thing? *Curr. Opin. Biotechnol.* **22**, 527–532.

Urankar, R. N., Lust, R. M., Mann, E., Katwa, P., Wang, X., Podila, R., Hilderbrand, S. C., Harrison, B. S., Chen, P., Ke, P. C., *et al.* (2012). Expansion of cardiac ischemia/reperfusion injury after instillation of three forms of multi-walled carbon nanotubes. *Part. Fibre Toxicol.* **9**, 38.

Utell, M. J., Frampton, M. W., Zareba, W., Devlin, R. B., and Cascio, W. E. (2002). Cardiovascular effects associated with air pollution: Potential mechanisms and methods of testing. *Inhal. Toxicol.* **14**, 1231–1247.

Wingard, C. J., Walters, D. M., Cathey, B. L., Hilderbrand, S. C., Katwa, P., Lin, S., Ke, P. C., Podila, R., Rao, A., Lust, R. M., *et al.* (2011). Mast cells contribute to altered vascular reactivity and ischemia-reperfusion injury following cerium oxide nanoparticle instillation. *Nanotoxicology.* **5**, 531–545.